NONLINEAR BEHAVIOUR OF ONE-SIDE COATED PAPER: STATIC AND DYNAMIC VISCOELASTIC PROPERTIES

KLEMEN MOŽINA, STANISLAV PRAČEK and VILI BUKOŠEK

University of Ljubljana, Faculty of Natural Sciences and Engineering, Department of Textiles, 5, Snežniška, P.O. Box 312, SI-1101 Ljubljana, Slovenia

Received December 21, 2012

The research presented in this paper is the result of a study on the dynamic and static viscoelastic properties of one-side coated papers for the purpose of offset printing. During their formation and the technological processes of coating and printing, paper substrates are exposed to various traction forces, which cause not only nonlinear time dependence, but also a permanent irreversible deformation. Paper, which is basically a composite material, also demonstrates viscoelastic properties. Viscoelastic materials characteristically adjust and respond to external forces, i.e. stresses and strains, in the form of a continuous rearrangement of molecular, supramolecular and other hierarchical morphological structures.

Keywords: static, dynamic viscoelasticity, strain relaxation, creep, DMS, coated paper

INTRODUCTION

Paper as a viscoelastic material with a crystalline and amorphous regions exhibits an elastic and plastic flow. The elastic region corresponds to the linear proportion between load and elongation.[1] The viscoelastic region, however, corresponds to a region where the response is no longer linear and becomes highly time dependent. Viscoelastic materials have one specific property, as they continue to rearrange the molecular segments to respond and adjust to the applied force.[2-4] Viscoelastic properties of paper are as follows: nonlinear region of load-elongation curve, continuing extension/creep under constant load, load-elongation curve varying with the rate of load or applied force, load tendency required for a constant elongation, which decreases with time, and immediate and delayed elastic effect and non-recoverable elongation of paper.[5] Due to the viscoelastic nature of paper, creep and stress relaxation are the two conditions that result from non-recoverable deformation. In the stress-strain tests, paper starts out as a purely elastic body and after 0.3-0.6%, i.e. experimentally measured values (ε_y), of strain, paper exhibits flow. If the load is held constant, paper will flow indefinitely until it breaks.[6,7] Paper creep occurs in printing, where the force is applied to the paper and then released. During transport and through the printing press, the web is subjected to a complicated mechanical loading history, as well as to dampening by water.[8]

THEORY OF VISCOELASTIC BEHAVIOUR

Paper as a material behaves, on the one hand, as a firm elastic substance, where Hooke's law is applied and, on the other hand, as a viscose matter corresponding to Newton's law. The viscoelastic nature of paper can therefore cause variability in test data.[2,5,6] A review of elasticity prior to discussing viscoelastic properties has a highly practical significance. Elasticity in solids is a function of interatomic forces and is closely related to the internal molecular structure, since in fully elastic materials, the deformation is recoverable. The modulus of elasticity is a transformation of Hooke's law, which makes the dimension independency by applying the force to a unit area and length. The modulus of elasticity is therefore the coefficient of proportionality and a quantitative statement of the material's ability to

react to the applied deformation, and it depends on the order of material crystallinity.[2,9-13]

Strain relaxation

Perez has developed a molecular model that sustains the analysis of α relaxation. The amorphous region is characterized on a nanometre scale, with density fluctuations (entropy and enthalpy), where larger mobility (local molecular motions) is perceived at maximum or minimum local density (free enthalpy).[14,15] The process of molecular diffusion is, on the other hand, hierarchically correlated. Around T_g, local and short distance motions are required for a molecular translation to occur, which allow more complex motions and usually these local motions are responsible for β relaxation.[16] Shear micro-domains are formed under the application of local shear stress. The model provides two main relationships: first, the average relaxation time for the α-process, which is temperature and microstructure dependent and second, the viscoelastic complex shear modulus, which is a function of temperature and frequency. The first correlation of temperature and microstructure is dependent upon molecular mobility and is written as:

$$\tau_{mol} = t_0 \left(\frac{\tau_\beta}{t_0} \right)^{1/\chi} \tag{1}$$

where:

τ_{mol} – molecular mobility,

χ – correlation parameter ($0 < \chi > 1$),

t_0 – scaling parameter.

The correlation effect is less important when χ is larger. The occurred movements have the same rate and are independent from each other when $\chi = 1$. Generally speaking, χ is an order parameter that is temperature dependent and below T_g ascendances on physical aging.[8]

The mechanical model describing the phenomenon of strain relaxation is the Maxwell model and is written as follows:

$$\frac{d\varepsilon}{dt} = \underbrace{\frac{1}{E} \times \frac{d\sigma}{dt}}_{\text{Hook}} + \underbrace{\frac{\sigma}{\eta}}_{\text{Newton}} \tag{2}$$

$\frac{d\varepsilon}{dt} = 0$ when the specimen is deformed. By considering that $\eta = \tau E$ Eq. 2 becomes:

$$\begin{aligned} \frac{d\varepsilon}{dt} &= \frac{1}{E} \times \frac{d\sigma}{dt} + \frac{\sigma}{\tau E} = 0 \;/ : \sigma \\ \frac{d\sigma}{\sigma} &\times \frac{1}{Edt} + \frac{1}{\tau E} = 0 \;/ \times Edt \\ \frac{d\sigma}{\sigma} &+ \frac{dt}{\tau} = 0 \\ \frac{d\sigma}{\sigma} &= d\ln\sigma = -\frac{dt}{\tau} \end{aligned} \tag{3}$$

With integration of σ_0 (start point of experiment) and $\sigma_{(t)}$ (relaxation of stress in a given time) and with division of starting strain (ε_0), we get Eq. 4:

$$\begin{aligned} \ln\sigma_{(t)} - \ln\sigma_0 &= -\frac{dt}{\tau} \\ \sigma_{(t)} &= \sigma_0 e^{-\frac{t}{\tau}} \;/ :\; \varepsilon_0 \\ \frac{\sigma_{(t)}}{\varepsilon_0} &= \frac{\sigma_0}{\varepsilon_0} \times e^{-\frac{t}{\tau}} \\ E_{(t)} &= E_0 \times e^{-\frac{t}{\tau}} \end{aligned} \tag{4}$$

Eq. 4 represents a modulus of strain relaxation ($E_{(t)}$) in time (t). As during the experiment, the exponent relaxation of force with only one Maxwell element does not correspond to the actual time correlation, the multi-element model known as the Maxwell-Weichert model (Maxwell

elements linked parallelly) is applied. It is known for the multi-element model that the total sum of individual element responses is according to the Boltzman superposition principle, represented in Eq. 5.[17]

$$E_{(t)} = \frac{\sigma_{(t)}}{\varepsilon_0} = \frac{\sigma_{1_{(0)}}}{\varepsilon_0} \times e^{-\frac{t}{\tau_1}} + \frac{\sigma_{2_{(0)}}}{\varepsilon_0} \times e^{-\frac{t}{\tau_2}} + \frac{\sigma_{3_{(0)}}}{\varepsilon_0} \times e^{-\frac{t}{\tau_3}} + \ldots + \frac{\sigma_{n_{(0)}}}{\varepsilon_0} \times e^{-\frac{t}{\tau_n}}$$

$$E_{(t)} = E_{1_{(0)}} \times e^{-\frac{t}{\tau_1}} + E_{2_{(0)}} \times e^{-\frac{t}{\tau_2}} + E_{3_{(0)}} \times e^{-\frac{t}{\tau_3}} + \ldots + E_{n_{(0)}} \times e^{-\frac{t}{\tau_n}} \quad (5)$$

$$E_{(t)} = \sum_{i=1}^{n} E \times e^{-\frac{t}{\tau_i}}$$

where:

$\sigma_{n_{(0)}}$ – stress of n-part in time 0,

$E_{n_{(0)}}$ – modulus of n-part in time 0.

Creep

Paper recovery from tensile deformation exhibits a combination of elastic, viscoelastic and plastic properties.[6] Paper shows high strength due to the wood fibre presence that has a complex microstructure and inelastic constituent behaviour, and consequently a complex time dependent response.[18,19] Creep resistance is unlike the ideal strength and elastic characteristics, which are directly dominated by the bond nature, sensitive to the lattice structure. According to the spatial pattern, three kind of a lattice defects can be observed.[20] The first is zero dimensional, e.g. vacancy, interstitial atoms and atom mixture; the second is one-dimensional dislocation and the third are two-dimensional defects (stacking fault and grain boundary).[4,21] The nature of paper recovery after a more or less extended deformation has a great theoretical and practical advantage. However, in the creep experiment, where more direct effects are detected, an increase of plastic deformation has a great impact on the processing, storage and end-use of paper.[6,22,23] Numerous equations have been developed to represent time dependent material deformation. Creep and recovery can be written as:[24]

$$\varepsilon(t) = K + m \ln \frac{t}{t_r} \quad (6)$$

where:

ε – strain at given time (t),

K, m – functions of applied stress (σ).

For simplicity, t_r is set to 1. In this case, K indicates strain at 1 ms (load) or recovery (unload). t = 0 corresponds to either loading (creep) or unloading (recovery) the specimen.

Numerical analysis of stress-strain diagram

For evaluation of viscoelastic properties, the DINARA© method, based on a stress-strain diagram, was developed.[25] Usual tension experiments give us record about the tension force and elongation (breaking elongation), but they do not provide information about continuous change in modulus and other viscoelastic properties during the entire measuring time. Characteristic viscoelastic quantities that define polymer properties are calculated from the first deviation (elastic modulus), second deviation (velocity of change in elastic modulus), and third deviation of average master stress-strain curve, the farthermost deviation values and integral of stress-strain function. The basic program scheme is composed of: construction of "working" stress-strain curve (with interpolation, the extent measured values are limited), integration, numerical deviation and calculation of curve, writing out and graphical value presentation, which defines the viscoelastic properties of the specimen. The six point Lagrange method (Eq. 7) is used for interpolation.[25,26]

$$f\left(x_0 + ph\right) = \sum_{i=-2}^{3} A_i f_i + R_5$$

$$\begin{aligned} f\left(x_0 + ph\right) = {} & \frac{-p\left(p^2 - 1\right) \times \left(p - 2\right) \times \left(p - 3\right)}{120} \times f_{-2} + \\ & \frac{p\left(p - 1\right) \times \left(p^2 - 4\right) \times \left(p - 3\right)}{24} \times f_{-1} - \\ & \frac{\left(p^2 - 1\right) \times \left(p^2 - 4\right) \times \left(p - 3\right)}{12} \times f_0 + \\ & \frac{p\left(p + 1\right) \times \left(p^2 - 4\right) \times \left(p - 3\right)}{12} \times f_1 - \\ & \frac{p\left(p^2 - 1\right) \times \left(p + 2\right) \times \left(p - 3\right)}{24} \times f_2 + \\ & \frac{p\left(p^2 - 1\right) \times \left(p^2 - 4\right)}{120} \times f_3 \end{aligned} \tag{7}$$

where:

$$p = \frac{x - x_0}{h} = \frac{\varepsilon - \varepsilon_0}{\Delta\varepsilon}$$

$\Delta\varepsilon$ – distance between point on abscise,
R – remain,
ε_0 – extension,
ε – extension value around interpolation is made and
F_i – function value at ε_i.

In the first part of the stress-strain interpolation curve, two points are expressed and written as:

$$\begin{aligned} f\left(x_0 + ph\right) &= \sum_{i=0}^{1} A_i f_i + R_1 \\ f\left(x_0 + ph\right) &= \left(1 - p\right) f_0 + p f_1 \end{aligned} \tag{8}$$

At the end of the curve, the three-point interpolation is applied, as written in Eq. 9:

$$\begin{aligned} f\left(x_0 + ph\right) &= \sum_{i=-1}^{1} A_i f_i + R_2 \\ f\left(x_0 + ph\right) &= \frac{p\left(p - 1\right)}{2} \times f_{-1} + \left(1 - p^2\right) \times f_0 + \frac{p\left(p + 1\right)}{2} \times f_1 \end{aligned} \tag{9}$$

In order to calculate viscoelastic properties, the "working" stress-strain curve must correspond to the measured curve ($R^2 = 1$). Therefore, it is smoothed with a five-point expression.[26]

$$\begin{aligned} f_0 &= \sum_{i=-2}^{2} A_i f_i + R_3 \\ f_0 &= \frac{f_{-2} + 4f_{-1} + 6f_0 + 4f_1 + f_2}{16} \end{aligned} \tag{10}$$

The smoothed master curve is then integrated and derivatives are obtained. With the expanded Simpson rule, the calculation of integrated function values is done, i.e. for i = 3, 5, 7 etc.

$$\int_{x_0}^{x_{2n}} f\left(x\right) dx = \frac{h}{3}\left[f_0 + 4\left(f_1 + f_3 + \ldots + f_{2n-2}\right) + 2\left(f_2 + f_4 + \ldots + f_{2n-2}\right) + f_{2n}\right] \tag{11}$$

and for i = 2, 4, 6 etc.

$$\int_{x_0}^{x} f(x)\,dx = \frac{3h}{8}\left[f_0 + 2\left(f_3 + f_6 + \ldots + f_{n-3}\right) + 3\left(f_1 + f_2 + f_4 + \ldots + f_{n-1}\right) + f_n\right] \quad (12)$$

The first derivative of the master stress-strain curve is calculated on the basis of a five-point method, while the second and the third are as follows:

$$f'(x+ph) = \frac{1}{h}\left(\frac{2p^3 - 2p^2 - p + 1}{12} \times f_{-2} - \frac{4p^3 - 3p^2 - 8p + 4}{6} \times f_{-1} + \frac{2p^3 - 5p}{2} \times f_0 - \frac{4p^3 + 3p^2 - 8p - 4}{6} \times f_1 + \frac{2p^3 + 3p^2 - p - 1}{12} \times f_2\right) \quad (13)$$

The results of the numerical analysis of the stress-strain diagram are represented with the minimal, maximal and zero values function $\sigma = f(\varepsilon)$.[25,26]

Dynamic mechanical spectroscopy (DMS)

The DMS method presents substantially more information about viscoelastic properties than can be obtained from studying the time dependent changes caused by constant deformation (force relaxation) or constant force (creep).[17] The dynamic mechanical spectroscopy was measured by Rheovibron, enabling the measurement of direct dynamic loss tangent (tagδ) and from the scale calculation of dynamic elasticity. Moreover, it provides dynamic viscoelastic temperature dependence under various temperatures in the heater vessel.[27] Viscoelastic materials exhibit time, i.e. phase shift between induced deformation and stress response. This is known as tangent of mechanical loss. The experiment is based on a periodical sine induced on a strip of paper (deformation (ε)), measuring its response (stress (σ)). The dynamical elastic modulus (E'), mechanical loss modulus (E'') and complex modulus (E^*) can be calculated from the amplitude of measured deformation and stress, as written in Eq. 14.

$$\begin{aligned} E^* &= E' + iE'' \\ E^* &= \sqrt{E'^2 + E''^2} \\ E' &= E^* \times \cos\delta \\ E'' &= E^* \times \sin\delta \\ \tan\delta &= \frac{E''}{E'} \end{aligned} \quad (14)$$

The calculation of moduli is based on the following relations:

$$E^* = \frac{\sigma}{\varepsilon};\ \text{where}\ \sigma = \frac{\Delta F}{P};\ \text{and}\ \varepsilon = \frac{\Delta l}{l} \quad (15)$$

$$E^* = \frac{\Delta F}{P} \times \frac{l}{\Delta l}$$

where:

ΔF – amplitude of force at break in [N], and it is half of sine load amplitude,

P – surface area,

Δl – deformation amplitude in [cm]; actual half value of sine amplitude deformation and

l – specimen length at measuring point.

The dynamic amplitude of breaking force (ΔF) and breaking deformation amplitude are expressed with Eqs. 16 and 17.

$$\Delta F = 0.1 \times \frac{10^3}{D} \times N = 10^2 \times \frac{N}{D} \quad (16)$$

$$\Delta l = 5 \times 10^{-3} \times A \times N \quad (17)$$

where:

N; A – proportional coefficients that are at tagδ = 30 dB equal 1 and are decreasing/increasing at increased/decreased region of tagδ coefficients, D – value of measured dynamic force and $0.1 \times N$; 5×10^{-3} cm – calibration values for force and deformation sensors.

If we consider both amplitudes (Eq. 18) and constant K (Eq. 19), which adjusts the clamp

oscillation error and the specimen form, we can then calculate the complex modulus (E^*).

$$E^* = \frac{2}{DA} \times \frac{1}{P} \times 10^8 \quad (18)$$

$$E^* = \frac{2}{\left(D - \mathrm{K}\right) \times A} \times \frac{1}{P} \times 10^8 \quad (19)$$

From the complex modulus (E^*), the dynamic modulus (E') is then calculated according to Eq. 20:

$$E' = E^* \times \cos\delta \quad (20)$$

and with Eq. 21, the modulus of mechanical loss (E'') is obtained:

$$E'' = E^* \times \sin\delta \quad (21)$$

Numerous readings and calculations of modulus, according to Eqs. 19, 20 and 21 in the measured temperature range, are processed with the interactive graphic result analyser computer program called RHEOVIBRON©.[28]

EXPERIMENTAL

Materials

To study the viscoelastic paper properties, three different kinds of wood-free paper were obtained from the production line. Paper composed of sulphate cellulose pulp of conifer tree (spruce), deciduous tree (eucalyptus) and of production rejects (mixture of spur and eucalyptus), was internally sized with synthetic size, based on alkyketendimer (AKD) in neutral pH media, and its surface was starched on a Billblade machine. The one-side coating (mixture of natural calcium carbonate, synthetic latex, water and auxiliary materials) was applied off-line and then glazed on a supercalender. The measurements were performed on uncoated (UN), off-line one-side coated (CO) and on the coated side printed (PR) paper. A five-colour Heidelberg SpeedMaster CD 102-5+LX offset printing machine, with an excluded varnishing part, was used for printing.

Methods

The methods were chosen on the basis of the plastic deformation characterization of morphology, structure and viscoelastic properties. For the analysis of static and dynamic viscoelastic properties of one-side coated paper, four methods were chosen, i.e. relaxation of strain, creep, numerical analysis of the stress-strain diagram (DINARA©) and dynamic mechanical spectroscopy (DMS).

Strain relaxation and inverse creep was performed on an Instron 6022 dynamometer with a clamp outset of 180 mm. In both studied cases, we used 20, 40 and 60% of "load". In the case of strain relaxation, these loads were done according to the breaking force and in the creep analysis, we used elongation at break.

The numerical analysis of the stress-strain diagram (DINARA©) gives an insight into the mechanical-physical properties of the paper, the method enabling the calculation of various modulus etc.

A dynamic mechanical spectroscopy (DMS) was performed on a Rheovibron DDV-II-C and the calculations were conducted with the RHEOVIBRON© computer program. Paper strips, 0.5 mm in width and 85.0 mm in length, were subjected to temperature (i.e. 14-240 °C) and two different frequencies (i.e. 11 Hz and 110 Hz).

RESULTS

Static viscoelastic properties

Strain relaxation

Paper resistance vs. external deformation can be seen in the diagram of force vs. time as a decline from the ordinate axis. The studied paper was exposed for 30 minutes to 20, 40 and 60% of breaking force. When making a comparison of strain relaxation diagrams for uncoated, coated and printed paper in MD (Fig. 1), the curve exhibits a plateau relatively instantly. In printed paper subjected to all three loads, i.e. 20, 40 and 60%, strain relaxation is the slowest, as the binding of paper components is in this case the highest. However, uncoated paper does not have any layers of coating and/or printing ink on it, and that is why paper strain relaxation is easier and quicker. Individual fibres in the fibre network are able to reorganize as a consequence of the response to the load and they can reach the energy equilibrium. Uncoated paper is more flexible, softer and willing. After 330 s, the curves of coated and printed paper start to move from each other as they flow one into another from the higher (60%) to the lower (40%) breaking force (Fig. 2). When comparing the strain relaxation in MD and in CD, we can point out that the relaxation time needed for each direction is reasonably different. The time required for the material to achieve a set load is due to higher extensions noticeably longer, which can be observed from the comparison of Fig. 1 and Fig. 2.

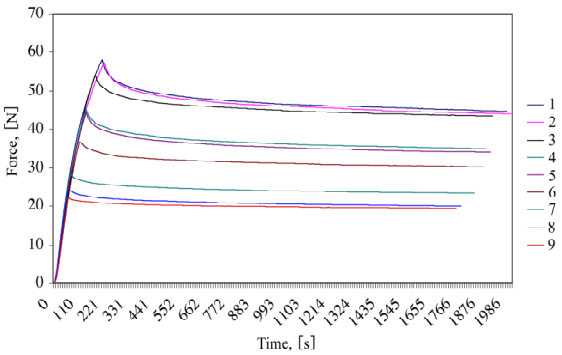

Figure 1: Strain relaxation of paper at 20%, 40% and 60% of a breaking force in MD (1–PR 60%, 2–CO 60%, 3–UN 60%, 4–PR 40%, 5–CO 40%, 6–UN 40%, 7–PR 20%, 8–CO 20%, 9–UN 20%)

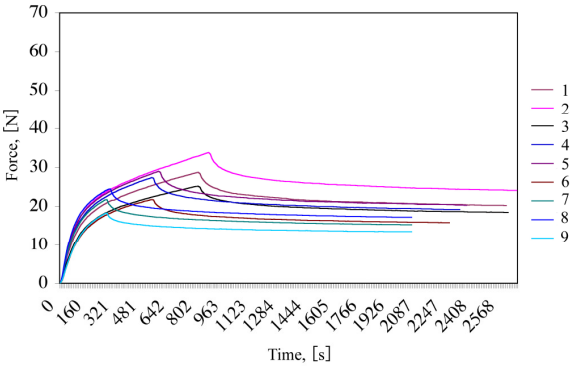

Figure 2: Strain relaxation of paper at 20%, 40% and 60% of a breaking force in CD (1–PR 60%, 2–CO 60%, 3–UN 60%, 4–PR 40%, 5–CO 40%, 6–UN 40%, 7–PR 20%, 8–CO 20%, 9–UN 20%)

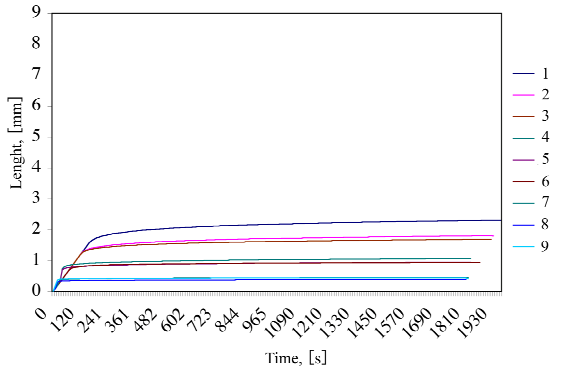

Figure 3: Creep of paper in MD at 20%, 40% and 60% of elongation at break (1–PR 60%, 2–CO 60%, 3–UN 60%, 4–PR 40%, 5–CO 40%, 6–UN 40%, 7–PR 20%, 8–CO 20%, 9–UN 20%)

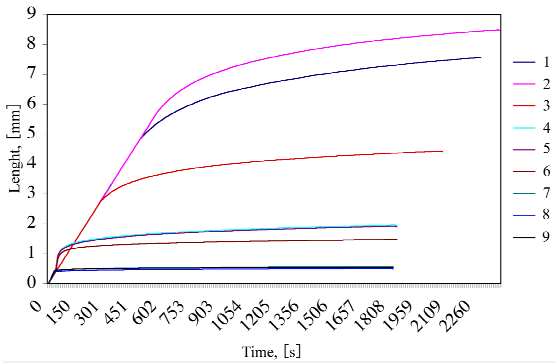

Figure 4: Creep of paper in CD at 20%, 40% and 60% of elongation at break (1–PR 60%, 2–CO 60%, 3–UN 60%, 4–PR 40%, 5–CO 40%, 6–UN 40%, 7–PR 20%, 8–CO 20%, 9–UN 20%)

Creep

Creep is defined as the material extension at constant load. Paper subjected to load for a longer time will try with a structural rearrangement to withstand or decrease the applied load. During the creep, the fibres rearrange and transfer within the disposable volume. The change in length is perceived as prolongation of specimen and it is more noticeable in CD. The time period of the test was the same, due to the analogy with the relaxation of strain, i.e. 30 min. Printed paper is more exposed to creep, as it is also to relaxation of strain in MD (Fig. 1). It extends by 2.31 mm or 1.28% (Fig. 3). On the other hand, the highest extension exceeds coated paper, which is subjected to extension at constant load (creep). It extends by 8.47 mm or 4.71% (Fig. 4). If we calculate from the experimental data the area of permanent deformation, which is between 2.00 mm^2 and 3.75 mm^2, we can conclude that the variation at constant load is not unnoticeable. In fact, it is high enough to be perceived by a human eye. At that range of plastic deformation, print quality is in question. The deviation in raster size or colour shade becomes obvious.

Numerical analysis of stress-strain diagram

The exact difference in the viscoelastic properties of different types of paper is calculated with a numerical analysis of strain, including the calculation of stress, modulus and its extensions. For the calculation, we used the computer program DINARA©.[17] The measurement results are presented in Table 1 and Figs. 5-10. A numerical analysis of the stress-strain curve describes the obvious differences in the viscoelastic properties among uncoated, coated and printed paper. They are visible in dissimilar modulus and its deformations, as well as in the velocity of changing moduli, such as E_i (initial modulus), E_y (Young's modulus), E_{yp} (yield modulus), E_0 (modulus at first turning point (the

highest modulus until yield point)), E_1 (modulus at second turning point (the lowest modulus of plastic region)) and E_3 (quickest decline in modulus) (Table 1).

DINARA© allows to calculate specific stress and extension at yield point, as these calculations are performed through the entire range of deformations until break and they represent a border between the elastic and plastic deformation. Specific stress (σ_y) and extension (ε_y) at yield point represent upper stress and extension limit until paper properties change noticeably. In comparison with uncoated paper, the coated one has a higher σ_y in MD by 2.79 MPa and in CD by 4.39 MPa. Printed paper has a higher σ_y in MD by 5.23 MPa and in CD by 2.23 MPa. On the other hand, among uncoated, coated and printed paper ε_y is less different. For instance, in CD, the uncoated and coated papers have the same calculated value of extension at the yield point, i.e. 0.59% (Table 1 and Figs. 6 and 8).

Table 1
Values of numerical analysis of stress-strain diagram

Measured parameter	Unit	Uncoated–UN		Coated–CO		Printed–PR	
		MD	CD	MD	CD	MD	CD
σ_p	MPa	58.03	29.05	71.03	42.74	80.27	39.27
ε_p	%	1.67	7.50	2.00	8.02	1.92	7.50
σ_y	MPa	17.67	7.19	20.46	11.58	22.90	9.61
ε_y	%	0.35	0.59	0.33	0.59	0.36	0.61
A_{sp}	J/kg	5.83×10^5	1.54×10^6	8.95×10^5	2.39×10^6	9.28×10^5	2.11×10^6
f_A		0.60	0.69	0.63	0.70	0.60	0.72
A_{sy}	J/kg	2.61×10^4	1.81×10^4	2.96×10^4	2.86×10^4	3.43×10^4	2.14×10^4
A_{el}	%	4.48	1.20	3.31	1.20	3.70	1.02
E_i	GPa	1.39	0.88	2.06	1.38	3.00	0.60
E_y	GPa	6.14	1.27	7.57	1.90	7.68	1.67
E_{yp}	GPa	5.78	1.48	6.59	2.36	7.46	2.34
E_0	GPa	6.42	1.60	7.65	2.72	8.23	2.62
ε_0	%	0.23	0.49	0.19	0.49	0.25	0.51
E_1	GPa	3.13	0.19	2.79	2.27	2.59	0.25
ε_1	%	0.79	1.65	0.76	1.31	0.77	1.53
E_3	GPa/%	– 6.67	– 1.63	– 9.71	– 4.05	– 10.09	– 2.76
ε_3	%	0.35	0.59	0.33	0.59	0.36	0.61

σ_p – specific stress, ε_p – specific strain, σ_y – specific stress at yield point, ε_y – specific strain at yield point, A_{sp} – specific breaking work, f_A – factor of breaking work, A_{sy} – specific breaking work at yield point, A_{el} – percentage of breaking work, E_i – initial modulus, E_y – Young's modulus, E_{yp} – yield modulus, E_0 – modulus at first turning point, ε_0 – strain at first turning point, E_1 – modulus at the second turning point, ε_1 – strain at the second turning point, E_3 – quickest decline in modulus, ε_3 – quickest decline in strain

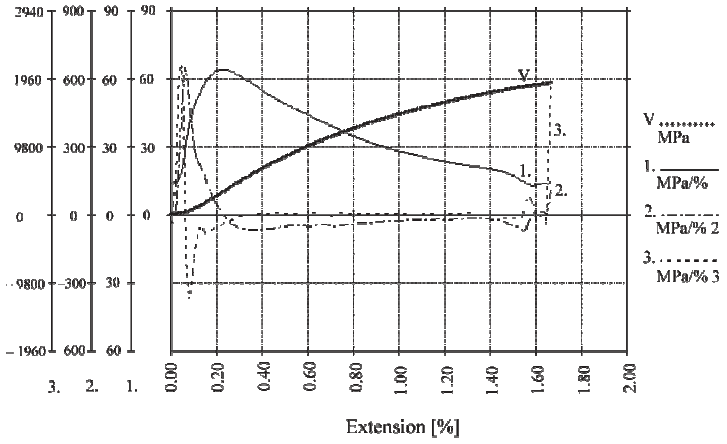

Figure 5: Stress-strain diagram for uncoated paper in MD

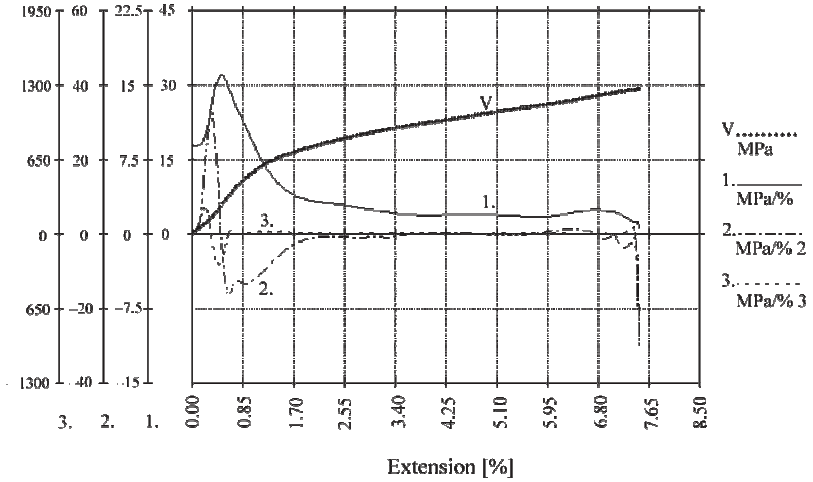

Figure 6: Stress-strain diagram for uncoated paper in CD

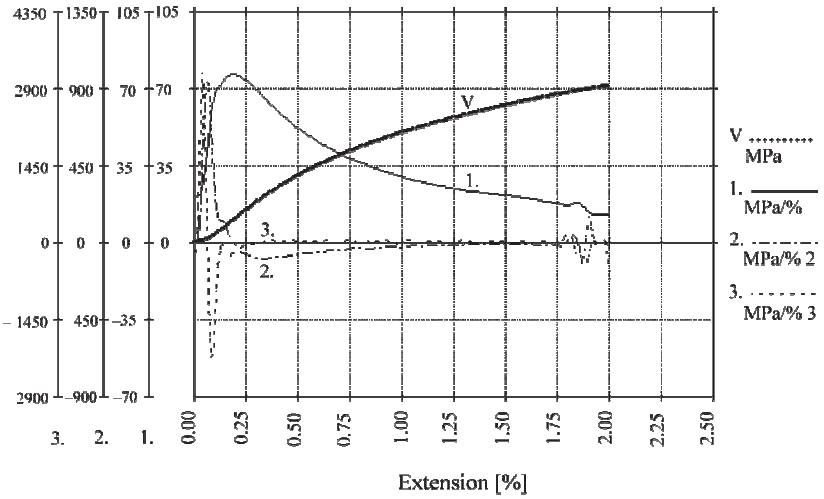

Figure 7: Stress-strain diagram for coated paper in MD

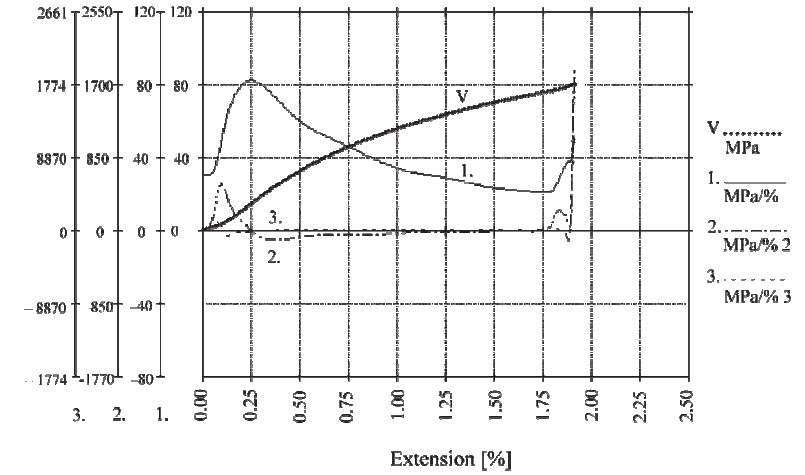

Figure 8: Stress-strain diagram for coated paper in CD

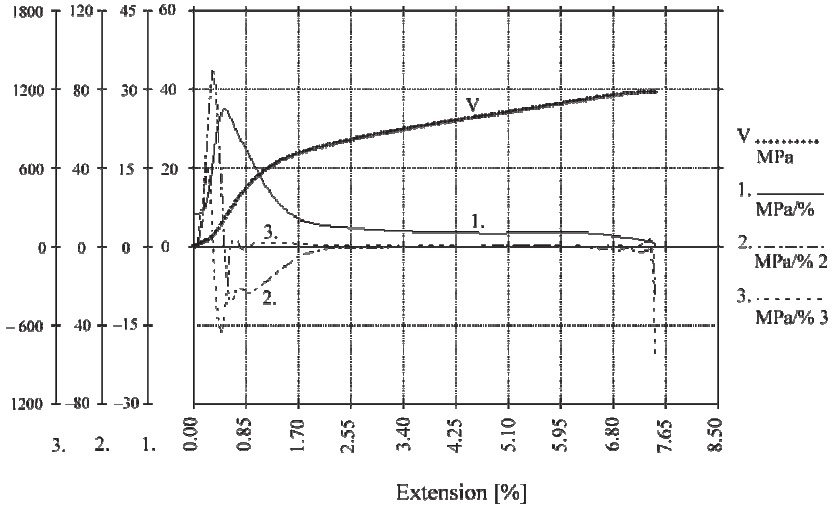

Figure 9: Stress-strain diagram for printed paper in MD

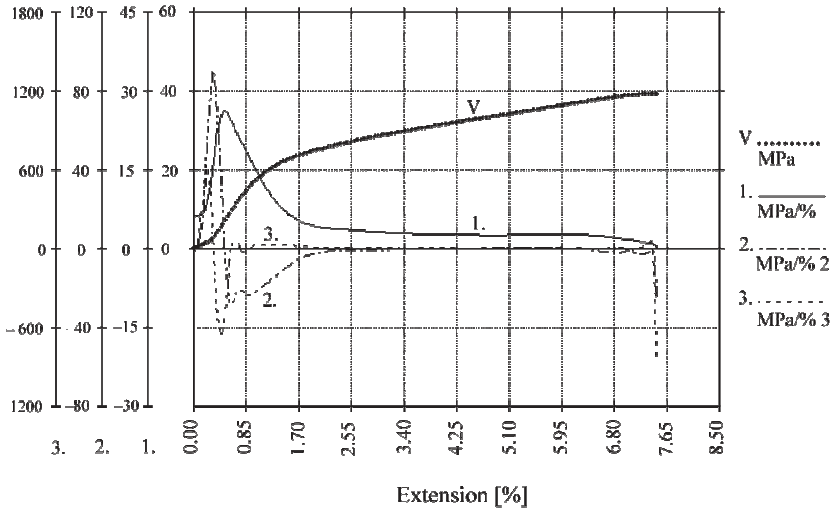

Figure 10: Stress-strain diagram for printed paper in CD

The results of the numerical analysis of stress-strain diagrams indicate and confirm the relaxation of strain and creep measurement that with each applied layer on the paper surface, the measured values increase and that in CD, the measured values are for the coated paper the highest among all three studied papers and are decreasing after offset printing. The initial modulus (E_i) is for uncoated paper 0.88 GPa, for coated 1.38 GPa and for printed 0.60 GPa (Table 1).

Dynamic viscoelastic properties

Dynamic mechanical spectroscopy (DMS)

The viscoelastic properties of paper can also be determined by dynamic viscoelastic spectroscopy. The results represent the viscoelastic behaviour of paper in a wide temperature range (14-240 °C), where the structure of paper is not changed considerably. The high structural stability is a desired property during the technological stages of completion, predominantly in the drying section. Although paper is not held at high temperature for a longer period of time, it has to be highly stable to temperature, especially for the electronic type of printing (digital and laser printing). The results for the studied papers show (Table 2 and Figs. 11-14) that due to the high structural stability, paper turned out well after the hot air drying. With the DMS method, at two different frequencies (11 Hz and 110 Hz), we analysed the dynamic

viscoelastic modulus (E′), loss in mechanical modulus (E″) and tangent of loss in the mechanical modulus (tagδ) before and after offset printing. In viscoelastic materials, a time shift or so-called phase shift exists between inerter deformation (ε) and response stress (σ). The results of DMS are presented in Table 2 and in Figs. 11-14.

Table 2
Results of interactive analysis of dynamic mechanical spectroscopy (DMS)

f [Hz]	Fibre direction	Value	Unit	T [°C]								
				25			100			200		
				UN	CO	PR	UN	CO	PR	UN	CO	PR
110	MD	E′	GPa	7.08	7.08	7.64	6.81	6.81	6.81	4.64	4.14	5.62
		E″	GPa	0.41	0.30	0.46	0.34	0.13	0.24	0.19	0.10	0.13
		tagδ	/	0.04	0.03	0.05	0.03	0.01	0.03	0.02	0.02	0.02
	CD	E′	GPa	3.04	7.08	5.41	2.71	6.07	4.47	2.07	4.14	3.16
		E″	GPa	0.10	0.50	0.38	0.06	0.15	0.15	0.05	0.12	0.10
		tagδ	/	0.03	0.04	0.05	0.02	0.02	0.02	0.02	0.02	0.02
11	MD	E′	GPa	6.56	5.41	5.41	5.41	4.47	5.41	3.83	4.64	5.01
		E″	GPa	0.23	0.41	0.17	0.14	0.12	0.08	0.11	0.13	0.11
		tagδ	/	0.03	0.04	0.03	0.02	0.01	0.02	0.02	0.01	0.02
	CD	E′	GPa	2.61	7.36	3.98	2.16	6.81	3.04	1.41	5.41	2.42
		E″	GPa	0.08	0.45	0.21	0.05	0.23	0.08	0.04	0.13	0.09
		tagδ	/	0.03	0.04	0.04	0.02	0.03	0.02	0.03	0.02	0.03

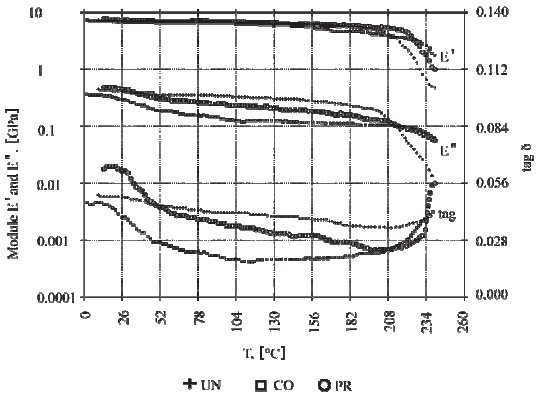

Figure 11: Paper dependence of E′, E″ and tagδ upon temperature in MD at 110 Hz

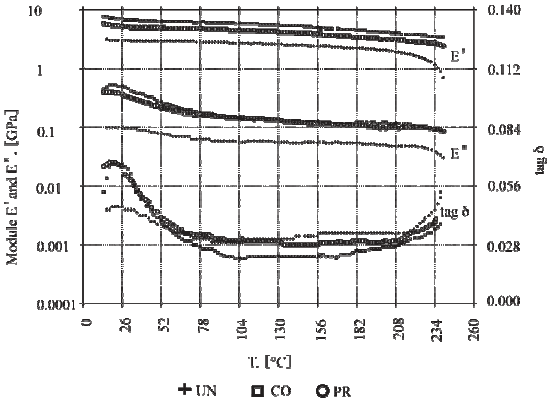

Figure 12: Paper dependence of E′, E″ and tagδ upon temperature in CD at 110 Hz

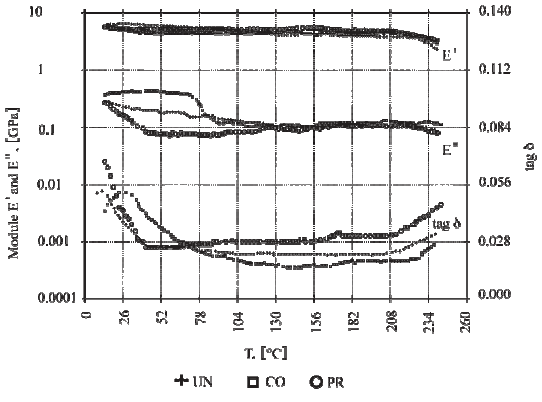

Figure 13: Paper dependence of E′, E″ and tagδ upon temperature in MD at 11 Hz

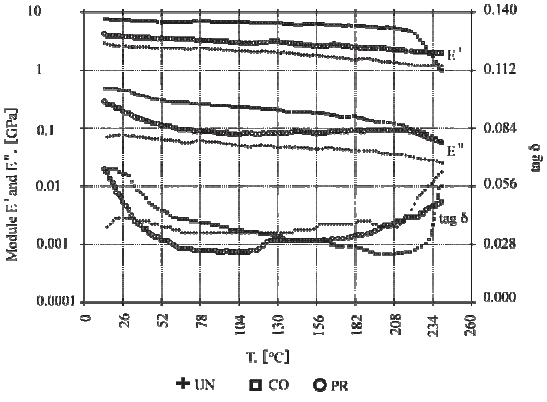

Figure 14: Paper dependence of E′, E″ and tagδ upon temperature in CD at 11 Hz

The measured viscoelastic values (Table 2) increase with frequency and its dependence is equal to temperature decreasing. A small distinction in dynamic viscoelastic properties (E′, E″ and tagδ) among the specimens, in MD and in CD, indicates the paper structural stability, irrespective of finishing stages.

For a paper manufacturer, the information on structural and temperature stability is very significant. The results of experimental research work of interactive analyses of dynamical mechanical spectroscopy, i.e. DMS, show a good relation with the theory. In the offset printing technique, it is a well-known fact that papers are fed in CD, due to the higher elastic region in comparison to MD. As seen from Table 2, at 11 Hz and 25 °C, an UN paper demonstrates a lower value of storage modulus (E′), e.g. 2.61 GPa, than a CO one, which attests 7.36 GPa. In the case of PR, paper exceeds another lowering to 3.98 GPa. The similarity in trend is also noticeable at two other temperatures (100 and 200 °C) and one frequency (110 Hz). The storage modulus is increased after the addition of paper coating as paper becomes more rigid and inflexible. After the printing, the storage modulus decreases due to the flex oil component in the offset printing ink, which acts as a lubricant and therefore increases paper willingness, resulting in fewer cracks in the coating layer, i.e. better printout quality.

CONCLUSION

Static viscoelastic properties and their indicators, e.g. modulus, stress-strain at yield point, specific work and relaxation time of the studied one-side coated papers are dependent upon the finishing process – flexibility drops after coating and slightly rises after printing, due to the influence of flax oil in the printing ink. On the other hand, dynamic viscoelastic properties, e.g. dynamic modulus, modulus of mechanical loss, tagδ, show a similar tendency towards static viscoelastic properties. The temperature dependence on dynamic viscoelastic properties up to 240 °C is not significant, which is a consequence of cellulose fibres and paper fillers that do not exceed any phase transitions and therefore sustain a rather stable structure in the wide temperature range. On the basis of the analysis of static viscoelastic properties, it can be concluded that printing reduces paper stiffness and does not change paper structure.

REFERENCES

[1] A. Dwan, *Journal of the American Institute for Conservation*, **26**, 1 (1987).

[2] E. P. Saliklis, in *Procs. The 11th Conference Engineering Mechanics Division/ASCE*, Florida, May 19-22, 1996, pp. 246-249.

[3] S. C. Xue and R. I. Tanner, *J. Non-Newton. Fluid Mech.*, **123**, 33 (2004).

[4] H. A. Ribeiro and C. A. V. Costa, *Chem. Eng. Sci.*, **62**, 6696 (2007).

[5] I. Heikkilä, *Pap. Puu-Pap. Tim.*, **79**, 186 (1997).

[6] J. Skowronski and A. A. Robertson, *J. Pulp Pap. Sci.*, **12**, 20 (1986).

[7] J. O. Lif, *Finite Elem. Anal. Des.*, **42**, 341 (2006).

[8] J. F. Blachot, L. Chazeau and J. Y. Cavaille, *Polymer*, **43**, 881 (2002).

[9] F. Cortés and M. J. Elejabarrieta, *Int. J. Solids Struct.*, **43**, 7721 (2006).

[10] A. S. R. Duarte, A. I. P. Miranda and P. J. Oliveira, *J. Non-Newton. Fluid Mech.*, **154**, 153 (2008).

[11] A. Miksic, J. Koivisto, J. Rosti and M. Alava, *Procedia Eng.*, **10**, 2678 (2011).

[12] J. Strömbro and P. Gudmundson, *Int. J. Solids Struct.*, **45**, 2420 (2008).

[13] J. J. M. Baltussen and M. G. Northolt, *Polymer*, **44**, 1957 (2003).

[14] Q. S. Xia, M. C. Boyce and D. M. Parks, *Int. J. Solids Struct.*, **39**, 4053 (2002).

[15] M. K. Ramasubramanian and Y. Wang, *Int. J. Solids Struct.*, **44**, 7615 (2007).

[16] K. Ho, *Int. J. Solids Struct.*, **46**, 1007 (2009).

[17] V. Bukošek, PhD Thesis, University of Ljubljana, 1997.

[18] L. O. Nordin and J. Varna, *Composites Part A*, **37**, 344 (2006).

[19] A. DeMaio and T. Patterson, *Mech. Mater.*, **40**, 133 (2008).

[20] J. Strömbro and P. Gudmundson, *Int. J. Solids Struct.*, **45**, 5765 (2008).

[21] Q. M. Hu and R. Yang, *Curr. Opin. Solid State Mater. Sci.*, **10**, 19 (2006).

[22] P. Isaksson, R. Hägglund, and P. Gradin, *Int. J. Solids Struct.*, **41**, 4731 (2004).

[23] C. Fellers and D. W. Coffin, in "Encyclopedia of Materials, Science and Technology", edited by K. H. J. Buschow *et al*., Elsevier Science Ltd., 2001, pp. 6720-6724.

[24] P. Rättö and M. Rigdahl, *Nordic Pulp Paper Res. J.*, **13**, 180 (1998).

[25] V. Bukošek, DINARA, Computer evaluation of viscoelastic properties of fibres, filaments, yarns, fabrics, ribbons, foils with tension test and flat products with pushing ball experiment: software, 1st ed., University of Ljubljana, 1989.

[26] M. Abramowitz and I. A. Stegun, in "Handbook of Mathematical Functions", 10th ed., edited by M.

Abramowitz and I. A. Stegun, Dover Publication Inc., 1972, pp. 877-899.
[27] Rheovibron, Direct Reading Dynamic Viscoelastometer, *Instruction Manual*, No. 68, Tokyo, Japan, 1973.
[28] V. Bukošek, Rheovibron, dynamic mechanic relaxation properties of oriented polymers – calculation and graphical evaluation, software, 1st ed., University of Ljubljana, 1989.